Journal of Hazardous Materials 172 (2009) 472–478

Contents lists available at ScienceDirect

Journal of Hazardous Materials

journal homepage: www.elsevier.com/locate/jhazmat

Simulataneous pentachlorophenol decomposition and granular activated carbon regeneration assisted by dielectric barrier discharge plasma

Guang-Zhou Qu[a], Na Lu[a,b], Jie Li[a,b,*], Yan Wu[a,b], Guo-Feng Li[a,b], Duan Li[a,b]

[a] Institute of Electrostatics and Special Power, Dalian University of Technology, Dalian 116024, PR China
[b] Key Laboratory of Industrial Ecology and Environmental Engineering, Ministry of Education, Dalian 116024, PR China

ARTICLE INFO

Article history:
Received 10 March 2009
Received in revised form 8 July 2009
Accepted 9 July 2009
Available online 16 July 2009

Keywords:
Granular activated carbon
Dielectric barrier discharge
Pentachlorophenol
Degradation

ABSTRACT

An integrated granular activated carbon (GAC) adsorption/dielectric barrier discharge (DBD) process was applied to the treatment of high concentration pentachlorophenol (PCP) wastewater. The PCP in water firstly was adsorbed onto GAC, and then the degradation of PCP and regeneration of exhausted GAC were simultaneously carried out by DBD. The degradation mechanisms and products of PCP loaded on GAC were analyzed by EDX, FT-IR and GC–MS. The results suggested that the C—Cl bonds in PCP adsorbed by GAC were cleaved by DBD plasma, and some dechlorination and dehydroxylation products were identified. The adsorption capacity of adsorption/DBD treated GAC could maintain relatively high level, which confirmed that DBD treatment regenerated the GAC for subsequent reuse. The adsorption of N_2, Boehm titration and XPS were used to investigate detailed surface characterizations of GAC. It could be found that DBD plasma not only increased the BET surface area and pore volume in micropore regions, but also had remarkably impact on the distribution of the oxygen-containing functional groups of GAC.

1. Introduction

Activated carbon (AC) is profusely used as an efficient and versatile adsorbent in decontamination processes because of its extended surface area, high adsorption capacity, developed porous structure and special surface reactivity [1–4]. However, the adsorption by AC is not the final pollutants disposal method, resulting only in the transition of the toxic organic substances from the liquid or gas phase to the solid phase. In addition, AC is relatively expensive and easily saturated; thus it would not only be uneconomic but also bring about environmental secondary pollution if the exhausted AC is not effectively treated [5]. Therefore, simultaneous degradation of pollutants adsorbed by AC and regeneration of exhausted AC appear to be considerable alternative which may be economically more attractive for a wider application of AC in pollution control processes.

The dielectric barrier discharge (DBD) was originally proposed by Siemens as far back as 1857. Since then, many research groups have investigated the feasibility of its various applications. Proposed uses include the sterilization of bacteria in soil [6], activation of polymers [7], cleaning and modification of material surface [8–10], and O_3 generation [11]. One of the most important uses of DBD plasma technology is in environmental pollution control because it can generate various active species (ions, radicals, O_3, etc.), which can rapidly react with most of the target compounds [12–15]. As people pay more attention to environmental-protection issues, DBD plasma technology alone cannot meet more and more strict standards for discharge of pollutants.

Accordingly, an integration of adsorption and discharge plasma decomposition has emerged as one of the most promising options for the treatment of contaminations due to the high degradation efficiency for pollutants and the reusability for adsorbent, and has been reported by some scientists recently [16–19]. But there is a little literature on DBD plasma to degrade organic pollutants loaded on AC and regenerate AC simultaneously. It has been reported that AC itself could accelerate the decomposition of O_3 to form higher oxidation potential •OH radicals under alkaline condition [20]. In the process of DBD, O_3 can be generated, which may be more effective for the oxidation of pollutants loaded on AC. Our previous work also suggested that DBD plasma could regenerate spent granular activated carbon (GAC) exhausted with dye [21]. Therefore, an integration of AC adsorption/DBD decomposition process may synergize the advantages of individual AC adsorption and DBD decomposition, as well as overcoming their respective limitations.

In this study, we designed a bench-scale experiment to investigate a facile water treatment technique, which integrated GAC adsorption and DBD plasma treatment for the removal of pentachlorophenol (PCP). Two main aspects were examined: the decomposition of PCP adsorbed by GAC from water and the regeneration of GAC for reuse. The two processes were successfully realized

* Corresponding author at: Institute of Electrostatics and Special Power, Dalian University of Technology, Dalian 116024, PR China. Tel.: +86 411 84708576; fax: +86 411 84708571.
E-mail address: lijie@dlut.edu.cn (J. Li).

0304-3894/$ – see front matter © 2009 Elsevier B.V. All rights reserved.
doi:10.1016/j.jhazmat.2009.07.035

simultaneously by the assistance of DBD plasma. PCP was chosen as target because of its high toxicity, persistence and bioaccumulation in aquatic organisms.

2. Experimental

2.1. Materials

The GAC (1.5 mm diameter, 3.0–5.0 mm length) used in this study was columned coal-based carbon and manufactured by Shenyang Chemical Reagent Factory, China. The GAC was pretreated as follows: firstly, the GAC was immersed in sodium hydroxide (0.1 mol L^{-1}) for 24 h, and then heated in boiling water for 30 min, washed with deionized water to remove fine particles and impurities, and lastly dried at 378 K for 24 h. The clean GAC was stored in a desiccator for use.

PCP (purity >95%) was purchased from the Chemical Plant of Nankai University. All other organic and inorganic reagents used were analytical grade (Tianjin Fuyu Fine Chemical Co., Ltd. and Shenyang Chemical Reagent Factory, China). Concentrated stock solutions of PCP were made by dissolving the PCP powder in 0.1 mol L^{-1} sodium hydroxide solution. Subsequent concentrations for experiments were obtained by diluting the stock solution with deionized water.

2.2. Methods

PCP loaded on GAC was obtained by mixing 400 mL of PCP solution (2000 mg L^{-1}) with 10.0 g pretreated GAC in 500 mL flasks. The flasks were sealed and placed in a thermostatic shaker (150 rpm, 298 K) for 4 days to obtain equilibrium.

The schematic diagram of the experimental apparatus was shown in Fig. 1. It mainly consisted of an alternating current high-voltage power supply and a DBD reactor. The frequency of the power supply was 200 Hz and the voltage was adjustable from 0 to 50 kV. The ground electrode of DBD reactor was round metal net, diameter was 60 mm. The GAC was filled on the ground net electrode. The discharge electrode (round thin metallic slice, thickness 2 mm, diameter 100 mm) was placed onto quartz barrier (foursquare thin quartz slice, thickness 2 mm, side length 150 mm). The gap space between the quartz barrier and ground net electrode was maintained at 6 mm. The O_2 was impregnated into the reactor to generate various active species. At terminal of the experiment setup, a bottle containing 50 mL of 10% KI solution was used to collect exhaust gas. The O_3 monitor (EG-2001, EBARA JITSUGYO) was used for the quantification of O_3 concentration from reactor.

2.3. Analysis

The determination of PCP concentrations in solution was performed by a HPLC using a Hypersil ODS (25 μm, 4.6 mm × 250 mm) reverse phase column, a methanol:water (1% acetic acid) = 0.9:0.1 mL min^{-1} of the mobile phase and UV detector (220 nm). The PCP residues on GAC were extracted in a conical flask using a 60 mL mixture of acetone and n-hexane (v/v = 1:1) with 1 mL of 37% hydrochloric acid added. The conical flask was kept shaking at 150 rpm for 60 min, and then ultrasonic extracting for 60 min. The extraction procedures were repeated for six times. Afterwards, the extract was evaporated in a water bath to incipient dryness. The resultant sample was dissolved in sodium hydroxide and analyzed by HPLC.

An Agilent 6890N gas chromatography (GC) coupled with an Agilent 5975 mass selective (MS) detector and a capillary column (30 m × 0.25 mm × 0.25 μm) were used for the identification of intermediates and decomposition products. The pretreatment method of sample before GC/MS analysis, as described above, the intermediates and decomposition products residues on GAC firstly should be extracted, and then be concentrated.

The composition of virgin, saturated and adsorption/DBD treated GAC was determined by energy-dispersive X-ray spectroscopy (EDX, NORAN system). The Fourier transform-infrared (FT-IR) spectroscopy was applied in the characterization of the chemical bonds of the GAC samples. Sample discs were prepared by mixing 1 mg of the samples with 500 mg of KBr in an agate mortar and scanned in a range from 4000 to 400 cm^{-1} using an EQUINOX55 spectrophotometer, 100 scans were taken at a resolution of 4 cm^{-1}.

The structural properties of GAC were obtained from the physical adsorption of N_2 at 77 K determined by a Quantachrome autosorb-1 adsorption apparatus. The surface area was calculated using the BET equation, micropore volume by the *t*-plot and micropore size distribution (PSD) by using the Dubinin–Radushkevich (DR) equation [22]. The total pore volume was estimated to be the liquid volume of nitrogen at a relative pressure of about 0.99. Before and after DBD treatment, the adsorption equilibrium isotherms of PCP on GAC were measured according to the method provided by Abdul and Campbell [23] for the evaluation of adsorption capacity. Various chemical functional groups of GAC surface were determined using the titration method of Boehm [24]. The pH values of the GAC samples were evaluated according to ASTM standard procedure D3838

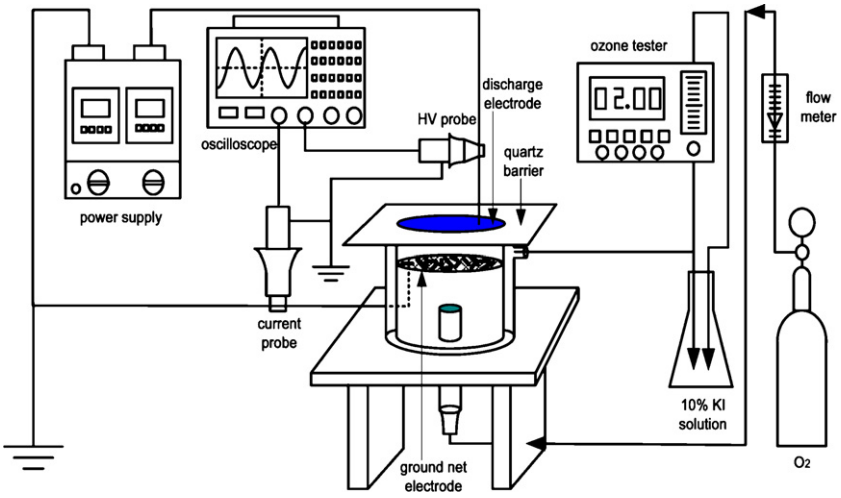

Fig. 1. Bench-scale apparatus of dielectric barrier discharge for PCP decomposition.

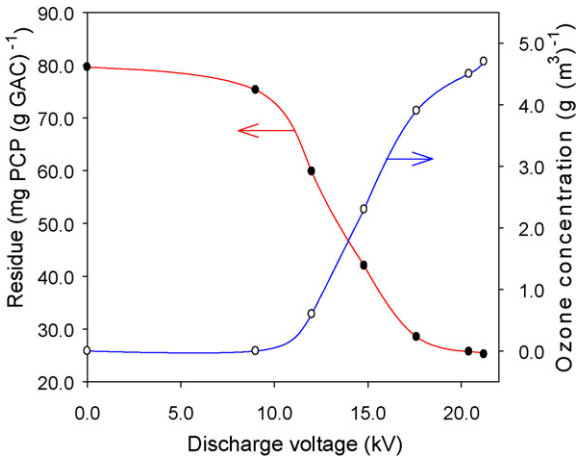

Fig. 2. The changes of PCP residues on GAC and O_3 concentration under different discharge voltages.

[25]. Briefly, 2.0 g of GAC was placed in 50 mL of hot water and boiled gently for 30 min, then the flash content was filtered, the cooled filtrate was measured by pH meter. X-ray photoelectron spectroscopy (XPS) analyses were conducted with an ESCALAB MK-II spectrometer (VG Scientific Ltd., UK) using AlKα radiation (1486.6 eV) with pass energy of 20 eV. A Shirley-type background was subtracted from the signals. After the baseline had been subtracted, the curve fitting was performed assuming a mixed Gaussian:Lorentzian peak shape. The components of the C_{1s} and O_{1s} peaks were fitted according to the model presented by Desimoni et al. [26] and Weitzsacker et al. [27].

3. Results and discussion

3.1. Decomposition of PCP loaded on GAC by DBD plasma

As mentioned above, DBD process can generate large numbers of active species (such as ions, radicals and O_3), ultraviolet light, heat and so on, which were directly relative to the discharge voltage [28]. Therefore, the discharge voltage was regarded as one of the most important parameters for the degradation of PCP loaded on GAC.

In this study, the investigated discharge voltage levels were 9.0, 12.0, 14.6, 17.6, 20.4 and 21.2 kV, and other parameters remained constant, namely, adsorption capacity of GAC for PCP 79.6 mg g^{-1}, power frequency 200 Hz, treatment time 60 min, treatment amount 2.0 g, water content of GAC 37.5% and 2 L min^{-1} O_2 was impregnated into the reactor (in following context, unless special conditions were required, all experiments were conducted at this condition, and discharge voltage was 20.4 kV). The results for PCP residues on GAC were plotted in Fig. 2. It was observed that PCP residues on GAC decreased with the increases of the discharge voltage.

In lower voltage, the concentration of O_3 was present in lower values in DBD with GAC. As the discharge voltage increased the O_3 concentration increased (Fig. 2). The results indicated that PCP residues on GAC were relative to O_3 concentration. As we have known, GAC itself could improve the decomposition of O_3 to yield free radicals, such as •OH, HO_2^-, O_2^-, and immobiled radicals GAC–O, GAC–O_3, and the catalytic effect of GAC was prominent, as expressed by the following (1)–(4) reactions [29–31]. They could react with adsorbed pollutants on GAC [20] and was sufficient for the rupture of chemical bonds of PCP:

$$O_3 + H_2O + 2e^- \leftrightarrows O_2 + 2OH^- \quad (1)$$

$$O_3 + GAC \leftrightarrows GAC{-}O + O_2 \rightarrow \ldots \rightarrow H_2O_2 \text{ or } HO_2^- \quad (2)$$

$$O_3 + GAC \rightarrow \ldots \rightarrow {}^{\bullet}OH \quad (3)$$

$$O_3 + GAC \rightarrow \ldots \rightarrow {}^{\bullet}H_2O \quad (4)$$

3.2. Degradation mechanism analysis

3.2.1. EDX analysis

Fig. 3 shows EDX of the virgin, saturated and adsorption/DBD treated GAC. No Cl peak was identified for virgin GAC, but higher Cl peak was found for the GAC exhausted with PCP. After the satu-

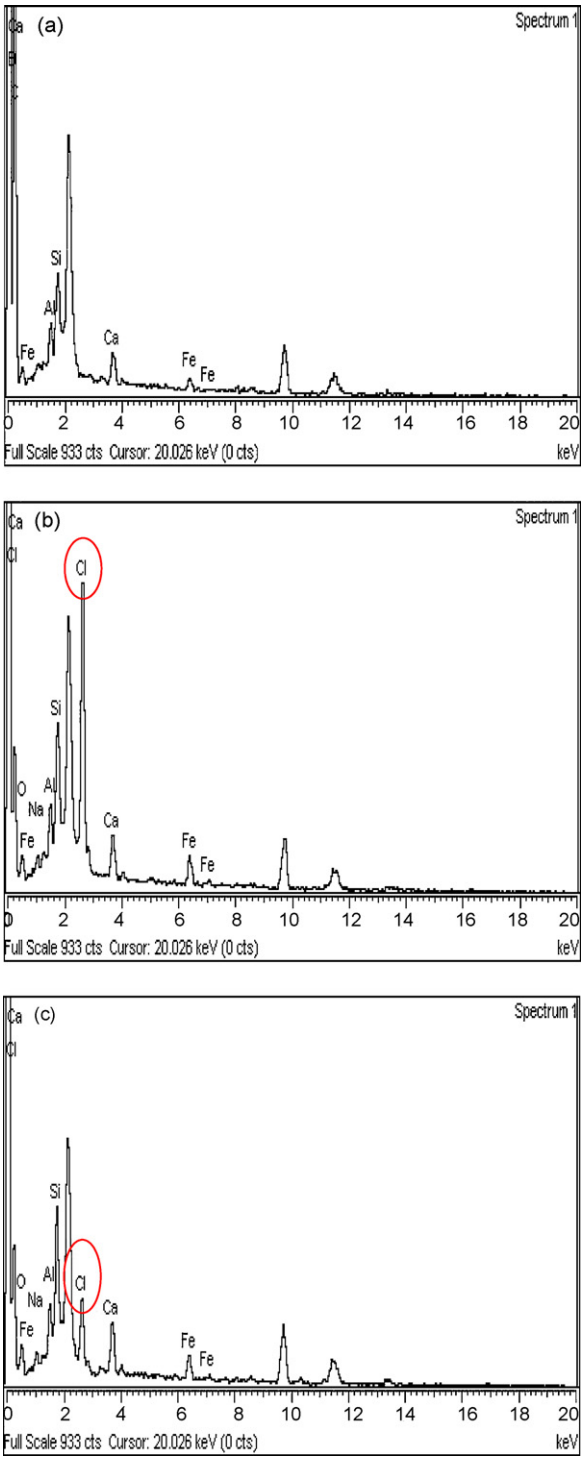

Fig. 3. Energy-dispersive X-ray spectroscopy of: (a) the virgin, (b) saturated and (c) adsorption/DBD treated GAC.

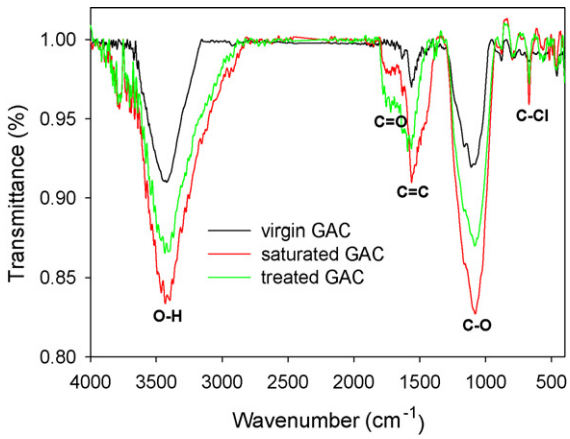

Fig. 4. FT-IR spectra of the virgin, saturated and adsorption/DBD treated GAC.

rated GAC was treated by DBD plasma, the Cl peak had a significant decreases, which indicated DBD plasma causing the dechlorination of PCP loaded on GAC.

3.2.2. FT-IR analysis

The transmission FT-IR spectrometry was applied for the characterization of the chemical bonds of the GAC surface. FT-IR spectra of the virgin, saturated GAC exhausted with PCP and adsorption/DBD treated GAC were depicted in Fig. 4. It could be noticed that the peaks at ~3440, ~1570 and ~1100 cm^{-1} appeared for all the GAC samples, which suggested that they possessed similar groups on their surface. The broad band centered at ~3440 cm^{-1} could be assigned to ν(O—H) stretching vibrations in water or phenolic hydroxyl groups associated by hydrogen bonds, carboxylic groups [32–34]. The band around 1570 cm^{-1} was mainly associated with the aromatic ring stretching of C=C groups [35]. The peak at ~1100 cm^{-1} was usually assigned to C—O stretches in lactonic, ether and phenol groups [34]. In ~3440, ~570 and ~1100 cm^{-1} regions, as shown in Fig. 4, the saturated GAC presented more pronounced bands than virgin GAC, but the peaks of GAC sample after DBD plasma treatment had an obvious decreases. It might be the reason that the PCP adsorbed on GAC could increase the O—H, C=C and C—O groups. After DBD plasma treatment, PCP was decomposed, therefore, the intensity of O—H, C=C and C—O groups decreased. The virgin GAC showed less bands around 1640–1750 cm^{-1}, which was usually caused by the stretching vibration of C=O in ketones, aldehydes and carboxyl groups [34–37], while they were less pronounced for the saturated GAC than that for treated carbon.

It was interesting to admit that ~670 cm^{-1} band, which was attributed to stretching vibration of Ar—Cl, strongly increased and slightly decreased in the spectra of saturated GAC and DBD plasma treated carbon, respectively. It was consistent with the results obtained by EDX, suggesting that the PCP on GAC was decomposed to be 4-chlorophenol, 3-chlorophenol, other phenols without chlorine, etc., which would be hereinafter confirmed.

3.2.3. Identification of intermediates by GC–MS

For the saturated GAC sample, PCP, chlorophenol ramifications and some impurity peaks were detected (Fig. 5(a)). When analyzing the GAC sample by DBD treatment for 60 min, the chromatographic peaks of components in the extraction were shown in Fig. 5(b). It was found that besides the components mentioned above, two main dechlorination intermediate products, tetrachlorophenol (TetraCP) and trichlorophenol (TriCP), were distinguished, and a minor amount of dehydroxylation products and trichlorobenzene (TriCB) was also identified, which was consistent with the results obtained by Liu et al. [38] and Anotai et al. [39]. While in treating *p*-chlorophenol with O_3, Andreozzi and Marotta [40] detected chloride, glyoxalic acid, maleic acid, formic acid and CO_2 as the final decomposition products. Shen et al. [41] found carboxylic acids in the courses of decomposition of *p*-chloronitrobenzene in water by ozonation. Thus it was deduced that part of PCP might be converted to CO_2 and various small molecule acids ultimately in our process.

3.3. The GAC regeneration by DBD plasma

In order to evaluate the adsorption capacity of PCP on GAC samples, the adsorption isotherms of PCP on virgin GAC and adsorption/DBD treated GAC were shown in Fig. 6. It was clear that the adsorption capacity of adsorption/DBD treated GAC could maintain relatively high level, which confirmed that DBD treatment regenerated the GAC for subsequent reuse, but was lower than that of virgin GAC. Our previous work also confirmed this point [21].

It was intuitively understandable that the adsorption of organic compounds onto GAC depended on its structural properties. Therefore, some relevant surface properties of virgin GAC and adsorption/DBD plasma treated GAC were summarized in Table 1. The adsorption/DBD treated GAC sample exhibited larger pore volume and specific surface area, especially micropore area. The result of the PSD measurement using the DR method provided the distribution of pores in the range 1–20 Å. The PSD of the two samples (Fig. 7) showed that the adsorption/DBD treated GAC had more micropores than virgin GAC.

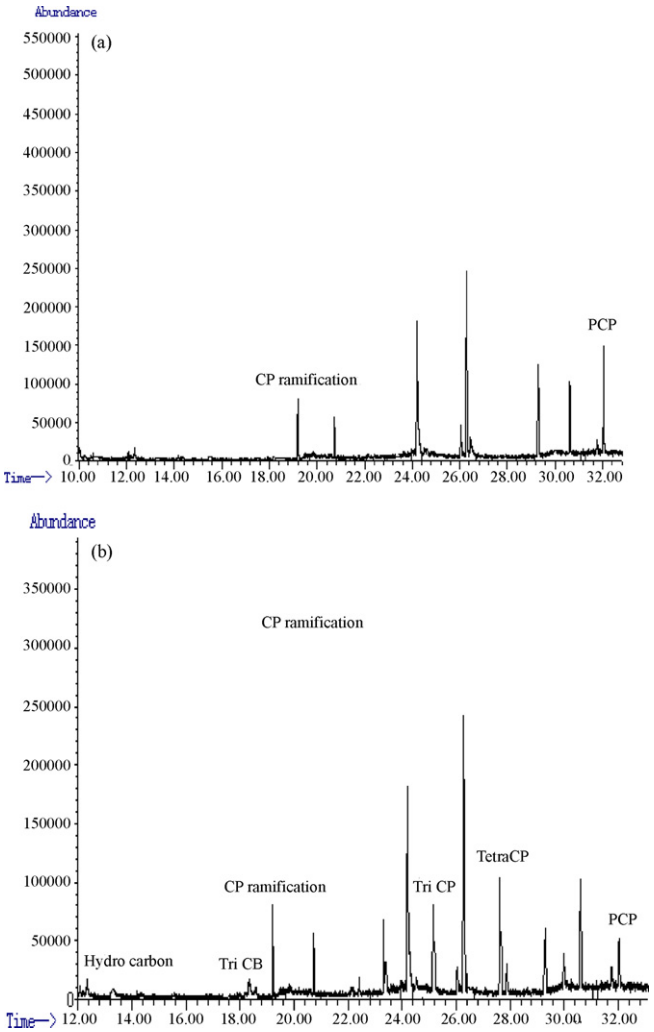

Fig. 5. Total ion chromatogram of components in extraction by GC–MS analysis: (a) saturated GAC and (b) adsorption/DBD treated GAC.

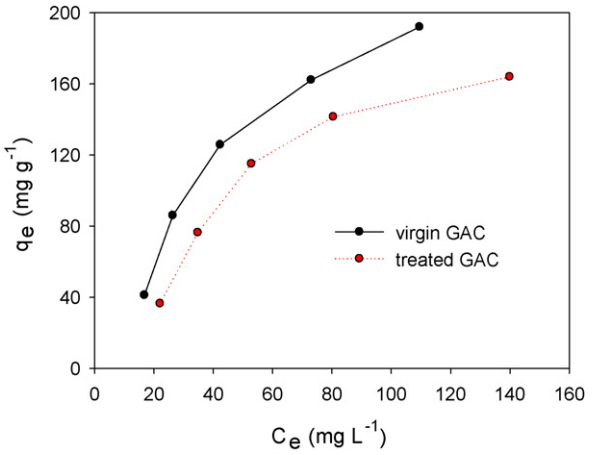

Fig. 6. Adsorption isotherms of virgin and adsorption/DBD treated GAC for PCP (temperature: 298 ± 1 K).

Table 1
Structural properties of the virgin and adsorption/DBD treated GAC samples.

GAC sample	S_{BET}	$S_{Micropore}$	$V_{Micropore}$	$V_{Total\ pore}$
	($m^2\ g^{-1}$)		($cm^3\ g^{-1}$)	
Virgin GAC	583.7	181.8	0.09	0.33
Treated GAC	657.3	421.9	0.20	0.37

One problem to be noted here was that the change of adsorption capacity was not consistent to change of surface properties of GAC. Besides the effect of residual PCP on the absorption capacity, there might be two reasons for this, on the one hand, it could be found that the change of specific surface area mainly attributed to micropore increase, the size exclusion between pore size of GAC and molecular size of PCP (~0.5 nm) maybe one of the reasons that caused adsorption capacity reduction, in addition. On the other hand, it was postulated that which might relate with the chemical functional groups of GAC.

Table 2 presents the results from titrations of the virgin and adsorption/DBD treated carbon together with the pH of the GAC samples in aqueous solution. It could be seen that the pH values of the GAC samples after plasma treatment decreased. The differences in surface chemistry of the GAC samples were clearly seen from the Boehm titration results presented in Table 2. After DBD plasma treatment, the amounts of phenolic and carboxylic groups on GAC sample increased, amounts of lactonic group decreased.

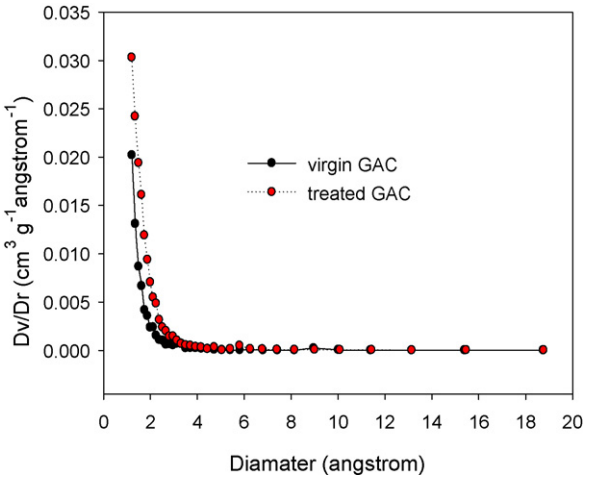

Fig. 7. Pore size distribution of virgin and adsorption/DBD treated GAC by DR method.

Table 2
Surface chemical properties of virgin and adsorption/DBD treated GAC samples (mmol g^{-1}).

Sample	pH	Carboxylic	Lactonic	Phenolic	Total acidic
Virgin GAC	8.65	0.350	0.015	0.260	0.625
Treated GAC	8.22	0.420	0.010	0.500	0.930

Table 3
Component peaks for C_{1s} region. XPS data for virgin and adsorption/DBD treated GAC samples.

Binding energy (eV)	Assignment	Virgin GAC (%)	Treated GAC (%)
284.7 ± 0.3	Graphitic carbon	53.6	49.1
286.0 ± 0.2	Carbon present in phenolic, alcohol or ether groups	29.9	23.8
287.4 ± 0.1	Carbonyl or quinone groups	9.1	12.9
289.0 ± 0.1	Carboxyl acidic groups	7.4	14.2

XPS was regarded as a useful tool for analyzing the surface properties of the sample including the distribution of functional groups. Fig. 8 shows the high-resolution C_{1s} and O_{1s} XPS spectra of the virgin and adsorption/DBD treated GAC. It could be seen that the C_{1s} spectra span over a broad energy range from 282.0 to 293.0 eV, which could be well fitted into four peaks for the virgin and adsorption/DBD treated GAC. The first peak at 284.7 eV was assigned to the carbon skeleton, and the second, the third and the fourth peaks at 286.0, 287.4 and 289.0 eV could be attributed to C—O, C=O and O—C=O bonds, respectively [42–45]. According to C_{1s} XPS spectra, the carbon skeleton and carbon presenting in phenolic, carbonylic or ester groups were the most numerous carbon-oxygen functional groups on the virgin and adsorption/DBD treated GAC.

The O_{1s} main peak of DBD treated GAC with PCP was broader than that of the virgin GAC and their centers were shifted from 532.1 to 533.3 eV. The O_{1s} subpeaks indicated the presence of several different species on virgin GAC and adsorption/DBD treated carbon, such as C=O (peak 1, binding energy (BE) = 531.0 eV), O=C—O ester groups (peaks 2, BE = 532.3 eV), O—C—O groups (peak 3, BE = 533.2 eV), and —C—O—H, O=C—O—H groups (peak 4, BE = 534.2 eV) [46–52].

The binding energy and relative content of carbon and oxygen from XPS survey spectra were also listed in Tables 3 and 4, respectively. The relative intensity of the peak at 284.7 and 286.0 eV decreased gradually, but the peak at 287.4 and 289.0 eV increased after DBD plasma treatment, implying that some carbon atoms in carbon skeleton were removed and some of the carbon atoms were functionalized through the creation of carbon—oxygen bonds. More information could be obtained from Table 4. After DBD treatment, the relative intensities of carbonyl and —C—O—H or O=C—O—H at 531.0 and 534.2 eV increased, whereas the relative intensities of ester and ether oxygen at 532.3 and 533.2 eV decreased, suggesting the formation of carboxyl and phenolic acidic groups, which was consistent with the results obtained by Boehm titration.

Several studies have documented that increasing the number of polar oxygen molecules within the carbon matrix or oxygen-

Table 4
Component peaks for O_{1s} region. XPS data for virgin and adsorption/DBD treated GAC samples.

Binding energy (eV)	Assignment	Virgin GAC (%)	Treated GAC (%)
531.0 ± 0.4	Carbonyl	11.1	21.5
532.3 ± 0.2	Ester	38.6	26.0
533.2 ± 0.1	Ether oxygen	34.8	21.1
534.2 ± 0.1	—C—O—H or O=C—O—H	15.5	31.4

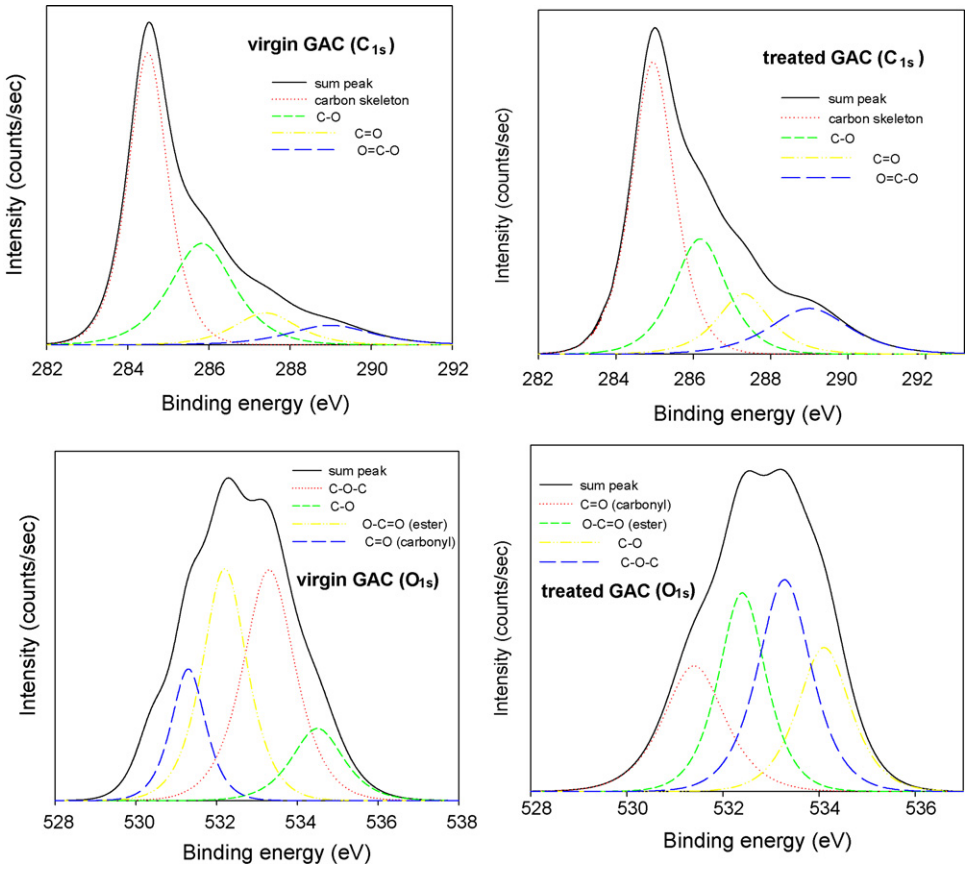

Fig. 8. C_{1s} and O_{1s} subpeaks of XPS spectra of the virgin and adsorption/DBD treated GAC.

containing surface acidity functional groups increased the polarity of carbon surfaces, and therefore their selectivity for water [53]. It has been further postulated that the adsorbed water clusters may block carbon pores and reduce adsorption capacity for hydrophobic compounds [54,55]. As a result, increases of carboxyl and phenolic acidic groups might be another reason why adsorption capacity of adsorption/DBD treated GAC was lower than that of virgin GAC.

4. Conclusions

An integrated GAC adsorption/DBD plasma process was adopted for the purification of PCP contaminated water. Most of the PCP adsorbed on GAC was decomposed into dechlorination and dehydroxylation intermediate products by DBD plasma. At the same time of PCP decomposition, GAC was regenerated by DBD plasma, and the adsorption capacity of adsorption/DBD treated GAC could maintain relatively high level. DBD plasma not only increased the BET surface area and pore volume in micropore regions, but also had remarkably impact on the distribution of the oxygen-containing functional groups of GAC, and increased the amounts of carboxyl and phenolic acidic groups of GAC surface. The integrated GAC adsorption/DBD plasma process has demonstrated its effectiveness for the removal of PCP from contaminated water and the regeneration of GAC, which has also provided us with an optimistic outlook for a pilot-scale experiment and even for the practical application of this process.

Acknowledgements

Financial supports provided by Ministry of Science and Technology, P.R. China (Project No. 2008AA06Z308) and Ministry of Education of the People's Republic of China (20070141004) are much gratefully acknowledged.

References

[1] D.M. Nevskaia, A. Santianes, V. Muñoz, A. Guerrero-Ruíz, Interaction of aqueous solutions of phenol with commercial activated carbons: an adsorption and kinetic study, Carbon 37 (1999) 1065–1074.
[2] S. Yenisoy-Karakas, A. Aygün, M. Günes, E. Tahtasakal, Physical and chemical characteristics of polymer-based spherical activated carbon and its ability to adsorb organics, Carbon 42 (2004) 477–484.
[3] C.T. Hsieh, H. Teng, Influence of mesopore volume and adsorbate size on adsorption capacities of activated carbons in aqueous solutions, Carbon 38 (2000) 863–869.
[4] M.M. Dubinin, V.V. Serpinsky, Isotherm equation for water vapor adsorption by microporous carbonaceous adsorbents, Carbon 19 (1981) 402–403.
[5] M.H. Zhou, L.C. Lei, Electrochemical regeneration of activated carbon loaded with *p*-nitrophenol in a fluidized electrochemical reactor, Electrochim. Acta 51 (2006) 4489–4496.
[6] M. Takayama, K. Ebihara, H. Stryczewska, T. Ikegami, Y. Gyoutoku, K. Kubo, M. Tachibana, Ozone generation by dielectric barrier discharge for soil sterilization, Thin Solid Films 506–507 (2006) 396–399.
[7] D.D. Pappas, A.A. Bujanda, J.A. Orlicki, R.E. Jensen, Chemical and morphological modification of polymers under a helium–oxygen dielectric barrier discharge, Surf. Coat. Technol. 203 (2008) 830–834.
[8] C.P. Klages, A. Hinze, K. Lachmann, C. Berger, J. Borris, M. Eichler, M. Hausen, A. von, M. Zänker, Thomas, Surface technology with cold microplasmas, Plasma Process. Polym. 4 (2007) 208–218.
[9] X. Xu, Dielectric barrier discharge-properties and applications, Thin Solid Films 390 (2001) 237–242.
[10] S. Kodama, H. Habaki, H. Sekiguchi, J. Kawasaki, Surface modification of adsorbents by dielectric barrier discharge, Thin Solid Films 407 (2002) 151–155.
[11] Z. Fang, Y.C. Qiu, Y.Z. Sun, H. Wang, K. Edmund, Experimental study on discharge characteristics and ozone generation of dielectric barrier discharge in a cylinder–cylinder reactor and a wire–cylinder reactor, J. Electrostat. 66 (2008) 421–426.
[12] K.P. Francke, H. Miessner, R. Rudolph, Plasma catalytic processes for environmental problems, Catal. Today 59 (2000) 411–416.

[13] J.L. Hueso, J. Cotrino, A. Caballero, J.P. Espinós, A.R. González-Elipe, Plasma catalysis with perovskite-type catalysts for the removal of NO and CH_4 from combustion exhausts, J. Catal. 247 (2007) 288–297.
[14] M. Magureanu, N.B. Mandache, P. Eloy, E.M. Gaigneaux, V.I. Parvulescu, Plasma-assisted catalysis for volatile organic compounds abatement, Appl. Catal. B 61 (2005) 12–20.
[15] A.G. Bubnov, E.Y. Burova, V.I. Grinevich, V.V. Rybkin, J.K. Kim, H.S. Choi, Plasma-catalytic decomposition of phenols in atmospheric pressure dielectric barrier discharge, Plasma Chem. Plasma Process. 26 (2006) 19–30.
[16] Y. Yamagata, K. Niho, K. Inoue, H. Okano, K. Muraoka, Decomposition of volatile organic compounds at low concentrations using combination of densification by zeolite adsorption and dielectric barrier discharge, Jpn. J. Appl. Phys. 45 (2006) 8251–8254.
[17] J.T. Yang, Y. Shi, W. Li, X. Wang, D.H. Wang, Combination of non-thermal plasma and activated carbon fibers for decomposition of hydrogen sulphide, Abstr. Pap. Am. Chem. Soc. 231 (2006) 148.
[18] T. Ohshima, T. Kondo, N. Kitajima, S.I. Mii, M. Sato, Decomposition of gaseous acetaldehyde using barrier discharge plasma with fibrous activated carbon as an electrode, J. Chem. Eng. Jpn. 40 (2007) 186–190.
[19] Y.Z. Zhang, J.T. Zheng, X.F. Qu, H.G. Chen, Effect of granular activated carbon on degradation of methyl orange when applied in combination with high-voltage pulse discharge, J. Colloid Interface Sci. 316 (2007) 523–530.
[20] P.C.C. Faria, J.J.M. Órfão, M.F.R. Pereira, Catalytic ozonation of sulfonated aromatic compounds in the presence of activated carbon, Appl. Catal. B 83 (2008) 150–159.
[21] G.Z. Qu, J. Li, Y. Wu, G.F. Li, D. Li, Regeneration of acid orange 7-exhausted granular activated carbon with dielectric barrier discharge plasma, Chem. Eng. J. 146 (2009) 168–173.
[22] S.J. Gregg, K.S.W. Sing, Adsorption, Surface Area, and Porosity, Academic Press, London, 1982, p. 90.
[23] H.M. Abdul, W.R. Campbell, Pentachlorophenol adsorption and desorption characteristics of granular activated carbon—1. Isotherms, Water Res. 30 (1996) 2901–2906.
[24] H.P. Boehm, Surface oxides on carbon and their analysis: a critical assessment, Carbon 40 (2002) 145–149.
[25] ASTM, Annual Book of ASTM Standards, Standard Test Method for pH of Activated Carbon, Philadelphia PA, D3838-80, 1996, pp. 531–532.
[26] E. Desimoni, G.I. Casella, A.M. Salvi, XPS/XAES study of carbon fibers during thermal annealing under UHV conditions, Carbon 30 (1992) 521–526.
[27] C.L. Weitzsacker, M. Xie, L.T. Drzal, Using XPS to investigate fiber/matrix chemical interactions in carbon–fiber-reinforced composites, Surf. Interface Anal. 25 (1997) 53–63.
[28] Y.S. Mok, J.O. Jo, H.J. Lee, Dielectric barrier discharge plasma-induced photocatalysis and ozonation for the treatment of wastewater, Plasma Sci. Technol. 10 (2008) 100–105.
[29] M. Sanchez-Polo, J. Rivera-Utrilla, Effect of the ozone-carbon reaction on the catalytic activity of activated carbon during the degradation of 1,3,6-naphthalenetrisulphonic acid with ozone, Carbon 41 (2003) 303–307.
[30] F.J. Beltrán, J.F. García-Araya, I. Giráldez, Gallic acid water ozonation using activated carbon, Appl. Catal. B 63 (2006) 249–259.
[31] P.M. Alvarez, J.F. Garcia-Araya, F.J. Beltran, I. Giraldez, J. Jaramillo, V. Gomez-Serrano, The influence of various factors on aqueous ozone decomposition by granular activated carbons and the development of a mechanistic approach, Carbon 44 (2006) 3102–3112.
[32] U. Zielke, K. Huttinger, W. Hoffman, Surface-oxidized carbon fibers: I. Surface structure and chemistry, Carbon 34 (1996) 983–988.
[33] P.M. Alvarez, J.F. Garcia-Araya, F.J. Beltran, F.J. Masa, F. Medina, Ozonation of activated carbons: effect on the adsorption of selected phenolic compounds from aqueous solutions, J. Colloid Interface Sci. 283 (2005) 503–512.
[34] P. Fanning, M. Vannice, A drifts study of the formation of surface groups on carbon by oxidation, Carbon 31 (1993) 721–730.
[35] C.L. Mangun, K.R. Benak, J. Economy, K.L. Foster, Surface chemistry, pore sizes and adsorption properties of activated carbon fibers and precursors treated with ammonia, Carbon 39 (2001) 1809–1820.
[36] C. Moreno-Castilla, M. López-Ramón, F. Carrasco-Maŕın, Changes in surface chemistry of activated carbons by wet oxidation, Carbon 38 (2000) 1995–2001.
[37] Y.P. Guo, D.A. Rockstraw, Physical and chemical properties of carbons synthesized from xylan, cellulose, and Kraft lignin by H_3PO_4 activation, Carbon 44 (2006) 1464–1475.
[38] X.T. Liu, X. Quan, L.L. Bo, S. Chen, Y.Z. Zhao, Simultaneous pentachlorophenol decomposition and granular activated carbon regeneration assisted by microwave irradiation, Carbon 42 (2004) 415–422.
[39] J. Anotai, R. Wuttipong, C. Visvanathan, Oxidation and detoxification of pentachlorophenol in aqueous phase by ozonation, J. Environ. Manage. 85 (2007) 345–349.
[40] R. Andreozzi, R. Marotta, Ozonation of *p*-chlorophenol in aqueous solution, J. Hazard. Mater. 69 (1999) 303–317.
[41] J.M. Shen, Z.L. Chen, Z.Z. Xu, X.Y. Li, B.B. Xu, F. Qi, Kinetics and mechanism of degradation of *p*-chloronitrobenzene in water by ozonation, J. Hazard. Mater. 152 (2008) 1325–1331.
[42] A.H. Yuwono, Y. Zhang, J. Wang, X.H. Zhang, H. Fan, W. Ji, Diblock copolymer templated nanohybrid thin films of highly ordered TiO_2 nanoparticle arrays in PMMA matrix, Chem. Mater. 18 (2006) 5876–5889.
[43] G. Beamson, D.T. Clark, D.S.L. Law, Electrical conductivity during XPS of heated PMMA: detection of core line and valence band tacticity effects, Surf. Interface Anal. 27 (1999) 76–86.
[44] Y.J. Zhu, N. Olson, T.P. Beebe, Surface chemical characterization of 2.5 μm particulates ($PM_{2.5}$) from air pollution in salt lake city using TOF-SIMS, XPS, and FTIR, Environ. Sci. Technol. 35 (2001) 3113–3121.
[45] W. Que, Y. Zhou, Y.L. Lam, Y.C. Chan, C.H. Kam, Preparation and characterizations of $SiO_2/TiO_2/\gamma$-glycidoxypropyltrimethoxysilane composite materials for optical wave guides, Appl. Phys. A 73 (2001) 171–176.
[46] C.D. Wagner, W.M. Riggs, L.E. Davis, J.F. Moulder, G.E. Muilenberg, Handbook of X-ray Photoelectron Spectroscopy, Perkin Elmer, Eden Prairie, MN, 1978.
[47] W.P. Yang, D. Costa, P. Marcus, Resistance to pitting and chemical composition of passive films of a Fe-17%Cr alloy in chloride-containing acid solution, J. Electrochem. Soc. 141 (1994) 2669–2676.
[48] S.D. Gardner, C.S.K. Singamsetty, G.L. Booth, G.R. He, C.U. Pittman, Surface characterization of carbon fibers using angle-resolved XPS and ISS, Carbon 33 (1995) 587–595.
[49] S. Biniak, G. Szymański, J. Siedlewski, A. Światkowski, The characterization of activated carbons with oxygen and nitrogen surface groups, Carbon 35 (1997) 1799–1810.
[50] J.F. Moulder, W.F. Stickle, P.E. Sobol, K. Bomben, in: J. Chastain (Ed.), Handbook of X-ray Photoelectron Spectroscopy, 2nd ed., Perkin-Elmer Corporation, Physical Electronics Division, Eden Prairie, MN, 1992.
[51] H.M. Ismail, D.A. Cadenhead, M.I. Zaki, Surface reactivity of iron oxide pigmentary powders toward atmospheric components: XPS and gravimetry of oxygen and water vapor adsorption, J. Colloid Interface Sci. 183 (1996) 320–328.
[52] P. Burg, P. Fydrych, D. Cagniant, G. Nanse, J. Bimer, A. Jankowska, The characterization of nitrogen-enriched activated carbons by IR, XPS and LSER methods, Carbon 40 (2002) 1521–1531.
[53] T. Karanfil, J. Kilduff, Role of granular activated carbon surface chemistry on the adsorption of organic compounds. 1. Priority pollutants, Environ. Sci. Technol. 33 (1999) 3217–3224.
[54] Y. Kaneko, M. Abe, K. Ogino, Adsorption characteristics of organic compounds dissolved in water on surface-improved activated carbon fibers, Colloid Surf. 37 (1989) 211–222.
[55] P. Pendleton, S.H. Wong, R. Shumann, G. Levay, R. Denoyel, J. Rouquerol, Properties of activated carbon controlling 2-methylisoborneol adsorption, Carbon 35 (1997) 1141–1149.